

# REVERSE ENGINEERING OF PUMP AS TURBINE FOR CFD ANALYSIS

JIŘÍ SOUČEK\*, EVA BÍLKOVÁ, PETR NOWAK

*Czech Technical University in Prague, Faculty of Civil Engineering, Department of Hydraulic Structures, Thákurova 2077/7, 166 29 Praha 6, Czech Republic*

\* corresponding author: `jiri.soucek.2@fsv.cvut.cz`

**ABSTRACT.** Reverse engineering (RE) using 3D scanning is already a relatively technologically simple and cost-effective method. For water turbines, this is particularly true for RE of larger machines. With microturbines, there is a lot of pressure to minimise costs, even at the cost of reduced accuracy. Using an existing micro-PAT (Pump as Turbine) as an example, we showed the approach to assessing these microturbines, starting with scanning the entire internal flow profile of the turbine, reconstructing the surface into a 3D model, and numerically assessing it using CFD (Computational Fluid Dynamics). A different approach is necessary compared to standard large machines, whose dimensions allow trouble-free scanning of the flow parts of the turbine. Using CFD, we assessed the reconstructed geometry of the PAT. Two significant findings were made: the importance of high-quality 3D scanning by combining several cheaper 3D scanners and the necessity for reliable in-situ measurements for a successful CFD validation. Our future focus involves optimising PAT runner geometry in turbine mode to enhance energy production at the site and, at the same time, eliminating existing cavitation.

**KEYWORDS:** Reverse engineering, 3D scanning, pump as turbine (PAT), CFD modelling.

## 1. INTRODUCTION

In Central and Western Europe, there are many small hydropower plants (up to 10 MW) and especially many micro hydropower plants with outputs of up to 100 kW. Most of these power plants contain older and less efficient turbines. Owners often do not have enough funding for the overall reconstruction of the power plant, sometimes not even the whole turbine technology. The solution is to change and modify the internal parts of the equipment to adapt to changing hydrological parameters and increase the efficiency of the equipment. This solution results in a substantial increase in energy production while also being financially feasible.

Pumps operating in PAT (Pump as Turbine) mode are often installed at these sites. The purchase price of a standard manufactured pump is often much lower than that of a classic turbine [1]. Using a pump as a turbine has several disadvantages. The hydraulic efficiency is usually up to 70 %, which is low [2]. Predicting the turbine mode behaviour based on the pump mode behaviour is also a challenge. Additionally, flow control is impossible without installing other elements such as a frequency converter for runner speed regulation [3].

Unfortunately, the smaller and older the machine, the more likely it is that the drawings will not be available. For this reason, it is necessary to reconstruct the given turbine geometry using 3D scanning. So-called reverse engineering (RE) is mainly used for larger machines (more than 1 MW of installed power) [4] and is quite costly. Therefore, our effort was directed towards using low-cost 3D scanners to make our effort

financially viable but as precise as possible.

For a high-quality and relatively inexpensive assessment of the machine, it is advisable to use numerical flow modelling (CFD – Computational fluid dynamics). The entire CFD assessment is a fundamental element for further decision-making, whether a total replacement of the technology is necessary, or it is economically advantageous to replace only specific parts of the machine unit [5].

In this article, we focus on the parameters assessment of the existing pump in turbine mode at a selected location of the existing small hydropower plant (SHPP). The goal is to quantify the current operating values of the selected unit (PAT) by reconstructing the unit set using RE and a subsequent CFD analysis. This result will serve as a basis for a future optimisation of a new runner with a much higher efficiency and eliminating cavitation.

## 2. METHODOLOGY

For a centrifugal pump used in turbine mode with an outlet diameter of 450 mm, the internal flow parts were scanned – the volute, the runner, and the very short draft tube. Parts of the intake pipe and the elbow part of the pipe after the draft tube were partly scanned from the outside due to inaccessibility, and partly, the geometry was subsequently taken from the drawings of the piping system.

This was followed by adjustments and cleaning of the measured cloud point and the subsequent reconstruction of the surfaces. After reconstructing the surfaces and supplementing the inlet and outlet parts



FIGURE 1. Original runner of the PAT (left) and the volute of the turbine (right).



FIGURE 2. Cloud point of the runner (left) and the volute of the turbine (right).

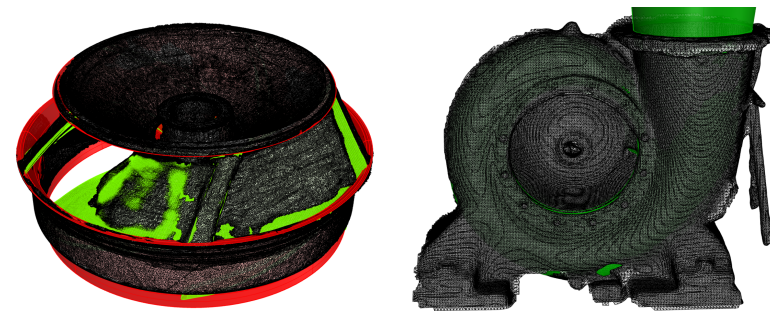


FIGURE 3. The reconstructed geometry of the runner (left) and the volute (right).

from the drawings, the entire 3D model of the equipment was available. This 3D model is further used for CFD modelling of the flow and subsequent evaluation of the hydraulic parameters of the turbine – especially the hydraulic efficiency  $\eta_h$ , head, velocities of the flow and Thoma's cavitation coefficient  $\sigma$ . There was a great effort to achieve a high-quality in-situ measurement. Unfortunately, due to the conditions on the site, only a very rough measurement could be performed, which certainly cannot be used to validate the CFD model.

### 3. REVERSE ENGINEERING

#### 3.1. 3D SCANNING AND DATA PROCESSING

Small machines require a different approach than large machines, that one can literally “crawl” through with a handheld scanner. Especially narrow blade channels, in our case with a width of around 100 mm (Figure 1 – left), are a big problem for high-quality scanning. Scanning the volute (Figure 1 – right) from the inside is also quite problematic. A scan of the internal and external surfaces was used, and the internal flow

surfaces were modelled when determining the wall thicknesses.

Several devices were combined to scan the turbine – Intel RealSense Lidar L515 [6, 7], Depth Camera D455 [7], and Depth Camera D405 were used for all parts, and an older professional Shining 3D EinScan Pro 2x scanner was used for additional scanning of the disassembled runner. After obtaining a point cloud from two scans (Figure 2), it was necessary to adjust these clouds. The merging and editing of the point clouds took place in the open-source program CloudCompare [8]. In this program, incorrect, deviating parts, or unnecessary scanned surrounding parts of the volute or runner surfaces were cleaned (or removed), and at the same time, the number of points in point clouds was reduced for more efficient work in surface reconstruction.

#### 3.2. 3D MODEL RECONSTRUCTION

Final adjustments and reconstruction to NURBS surfaces (Figure 3) were performed in the Rhinoceros program [9]. The exported and processed point clouds were stitched together and set to a characteristic posi-

tion in 3D (the  $z$ -axis passes through the shaft). As expected, the biggest challenge was correctly reconstructing the runner, specifically the runner passages, the leading and trailing edge blade geometries, and the gap between the front shroud and the wall. In addition to the obtained 3D scans, parts of the model, such as the inlet section and the parts after the draft tube outlet, had to be reconstructed from the drawings.

The differences between the scanned and reconstructed surfaces were verified for characteristic dimensions, such as the height of the entrance to the runner, inlet and outlet diameter of the runner and volute, chosen points on the leading edge and trailing edge of the runner, and several selected points on the pressure and suction sides of the blades. The average deviation of these verified points was up to 3 mm – with the fact that the main dimensions, such as input and output diameters, were within one millimetre of error compared to the scanned shape.

#### 4. IN-SITU MEASUREMENT

In general, there is a problem with older small hydropower plants in ensuring a sufficiently high quality in-situ measurement. Dismantling, removal, and measurement of existing older PAT devices in laboratory conditions is extremely costly and, therefore, unreachable. Due to the layout and state of the pipe elements, it was impossible to achieve a reliable measurement at our testing site. A very indicative measurement was therefore carried out, which could not be used for a comparison, let alone validation of the numerical model. The main problems were as follows:

- Old steel pipes with thick incrustations.
- Pipes with many bifurcations, inlet flap valve, confusers, and other elements generating hydraulic losses, especially considering high velocities over  $3 \text{ m s}^{-1}$ .
- There is no sufficiently straight section available for measuring pressure and flow that would meet the requirements of the standard IEC 62006 [10].
- The impossibility of installing a torque meter.

Discharge measurement was tested using a clamp-on ultrasonic flowmeter. Unfortunately, the value could not be measured due to rust incrustations on the DN 500 supply pipe. It was, therefore, necessary to take the discharge value from the KROHNE 800 W ultrasonic flowmeter, which is installed on the DN 1 400 bottom outlet, from which a pipe branch leads to this turbine. The read discharge value is  $0.65 \text{ m}^3 \text{ s}^{-1}$ . However due to the low average cross-sectional velocity of less than  $0.4 \text{ m s}^{-1}$ , there are, again, doubts about the magnitude of the error.

Existing pressure taps for pressure measurement are located in measuring sections. However, these sections are not always reliable for high-quality measurements according to IEC 62006 [10] (Figure 4). The inlet measuring section No. 1 before the volute is located  $2 \cdot D$

behind the elbow pipe segment and almost directly behind the flap valve. Pressure tap No. 2 is in the output measuring section of the very short draft tube, which is immediately followed by another elbow pipe segment. The pressure measurement was carried out by BD-Sensors DMP 331 electronic pressure transducers with a 4–20 mA current loop with an accuracy class of 0.25 %. The pressure values were logged within a period of 1 s. The measuring sections have the same cross-section. Therefore, the velocity head is also the same, so it is not necessary to include the velocity height. After subtracting the resulting pressure values, subtracting the height difference (exactly 1 m), and smoothing the measured pressure pulsations, the net head is equal to 13.80 m of the water column.



FIGURE 4. Locations of pressure taps.

Unfortunately, the torque on the shaft was not measured. Instead, the electric output power on the electrometer was read. At the same time, the efficiency of the generator and the losses between the turbine shaft and the wattmeter were determined (losses of 8%). In this way, the turbine power, or turbine efficiency, was calculated (Table 1).

Measured/read values	
Net head $H$ [m H <sub>2</sub> O]	13.80
Discharge $Q$ [m <sup>3</sup> s <sup>-1</sup> ]	0.65
Power output $P$ [kW]	59.0
Overall efficiency $\eta$	67.1 %
Calculated hydraulic efficiency $\eta_h$	72.9 %
$\eta_{11}$	92.1
$Q_{11}$	0.86

TABLE 1. Measured/read values.

## 5. CFD MODEL

Since it is not possible to measure the turbine parameters reliably enough, it is necessary to use numerical modelling methods. The goal is to simplify the model to the extent that it is possible to create a high-quality mesh, set boundary conditions, and replicate the actual hydraulic parameters of the turbine.

### 5.1. MESH

The entire 3D geometry was divided into a total of three parts (Figure 5), and a mesh was created for each of these parts:

- Part of the intake pipe and a volute – unstructured mesh,
- one blade passage of a runner – structured mesh,
- short draft tube and elbow pipe section – structured mesh.

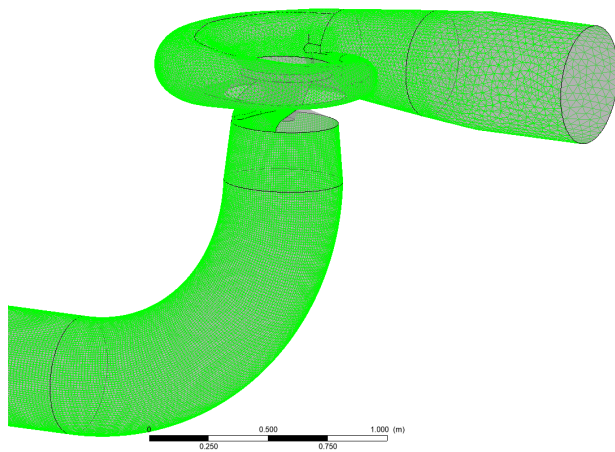


FIGURE 5. All three mesh parts.

The mesh was created in the ICEM CFD 2021 R1 program for the first and third parts of the model. The runner blade passage mesh was created in the Turbogrid® program. In general, the effort is to create the highest quality structured mesh. Due to the high geometry complexity in the area of the volute, we were forced to create a high-quality tetrahedral unstructured mesh with prismatic elements at the walls. In all three domains, including the rotation domain of the runner, the height of the first element near the wall was set so that the average value of  $y^+$  was around 100. In the case of the SST turbulence model, the first cell should be in the logarithmic boundary layer (recommended values of  $y^+$  are between 30 and 200) [11].

The GCI (Grid convergence index) was performed [12] for the estimated best efficiency point and with the numerical setup mentioned in the next chapter 5.2. Mesh dependency test for three meshes with a total of 0.7, 2, and 4 million cells was performed with output hydraulic efficiencies of 70.9%, 72.5%, and 73.0%, respectively. The GCI for two

finer grids equals 0.9%, which is sufficient according to Roache [13]. However, due to the many significant influences, such as the scanned surfaces and numerical setup, the medium mesh with two million elements was used.

### 5.2. NUMERICAL SETUP

The commercial Ansys CFX 2021 R1 software, which uses the finite volume method to solve RANS equations, was used for the calculation. A steady-state analysis of only one runner blade passage was performed with the use of rotational periodicity. The use of the whole runner was tested, but the output efficiency  $\eta_h$  and cavitation coefficient  $\sigma_s$  differed insignificantly. Transient calculation was not tested in this stage. An advection scheme, “High-resolution”, was used, which allows automatic switching between the second- and first-order numerical schemes. Between the static (volute and draft tube) domains and rotating (runner) domain, the Stage (“Mixing-plane”) of the general grid interface type [14] was used. This type of interface radially averages pressure, velocity, and turbulence values on one interface surface and transfers them to the other side of the interface. The walls are considered hydraulically smooth. A two-equation Shear Stress Transport turbulence model, originally introduced by Menter [15] as  $k - \omega$  SST, was used. This turbulence model is ordinarily used with variations in numerical simulations of rotating machines [16]. The upper boundary condition at the inlet to the model was set as the energy value (Total Pressure). The turbulence intensity  $I$  on the inlet is unknown, so it has been set to a default value of 5%. The lower boundary condition is set as the average static pressure. The rotational speed of a runner is set according to the eight-pole asynchronous generator to 760 rpm. The physical time step of the calculation is determined based on the angular velocity of a runner as  $0.5\omega^{-1}$ . During the calculation, we observe residuals and imbalances, but the most helpful is to monitor the behaviour of the hydraulic efficiency value. The behaviour of this value is the most indicative of the successful convergence of the calculation. We consider the calculation converged when the standard deviation of the efficiency for the last 50 iterations is below 0.1% (example in Figure 6).

## 6. EVALUATION OF CFD RESULTS

The resulting simulation values were evaluated in the Ansys CFD-Post environment. In addition to graphic outputs such as streamlines, two final values are fundamental for the evaluation – hydraulic efficiency  $\eta_h$  (not considering volumetric losses) and Thoma’s cavitation coefficient  $\sigma$  (more precisely, the  $\sigma_s$ , where the efficiency curve starts to drop below the level of efficiency in the cavitation free operation).

The simulation is defined in such a way that we are looking for the discharge and the hydraulic efficiency derived from the torque on the shaft for a given net

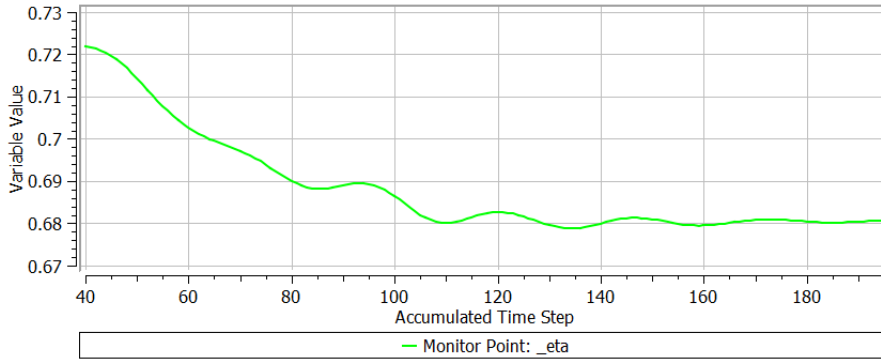


FIGURE 6. Example of the progress of the efficiency during the simulation.

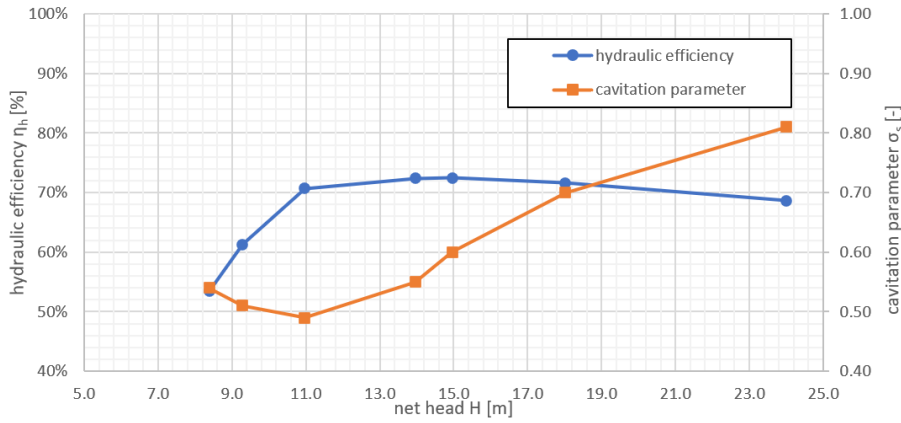


FIGURE 7. Dependency of hydraulic efficiency  $\eta_h$  and cavitation parameter  $\sigma_s$  on net head  $H$ .

PAT characteristics	OP2	OP3	OP4	OP5	OP6	OP7
Runner speed $n$ [rpm]	760	760	760	760	760	760
Net head $H$ [m H <sub>2</sub> O]	9.29	10.97	13.96	14.96	18.02	24.01
Discharge $Q$ [m <sup>3</sup> s <sup>-1</sup> ]	0.445	0.489	0.547	0.566	0.611	0.681
Shaft torque $M$ [N·m]	312	467	681	756	971	1382
Power output $P$ [kW]	24.8	37.2	54.2	60.2	77.3	110.0
Hydraulic efficiency $\eta_h$	61.3 %	70.7 %	72.4 %	72.5 %	71.6 %	68.6 %
Cavitation parameter $\sigma_s$	0.51	0.49	0.55	0.60	0.70	0.81
$n_{11}$	112.2	103.3	91.5	88.4	80.6	69.8
$Q_{11}$	0.72	0.73	0.72	0.72	0.71	0.69

TABLE 2. Simulated operational points of our PAT turbine.

head and a given turbine speed. The evaluation is done by the following formula:

$$\eta_h = \frac{P}{H \rho g Q} = \frac{M \omega}{H \rho g Q} = \frac{M n 2\pi}{H \rho g Q \cdot 60} \quad (1)$$

$$\frac{M_{11} n_{11} \pi}{Q_{11} \rho g \cdot 30} = \frac{P_{11}}{Q_{11} \rho g},$$

where  $\eta_h$  [-] is the hydraulic efficiency,  $H$  [m] is the net head calculated according to the IEC 62006 [10],  $Q$  [m<sup>3</sup> s<sup>-1</sup>] is the discharge value,  $\rho$  [kg m<sup>-3</sup>] is the density of water of 999.8 kg m<sup>-3</sup>,  $g$  [m s<sup>-2</sup>] is the gravitational constant of 9.807 m s<sup>-2</sup>,  $M$  [N m<sup>-1</sup>] is the shaft torque,  $\omega$  [rad s<sup>-1</sup>] is the angular velocity, and  $n$  [rpm] is the rotational velocity. The following are the

unit characteristics, which are recalculated values for a turbine with a diameter of 1 m and net head of 1 m. The turbine's unit torque is  $M_{11}$ , unit speed is  $n_{11}$ ; unit discharge is  $Q_{11}$ , and unit power output is  $P_{11}$ .

Table 2 shows the fundamental values subtracted from the numerical simulation for the selected points. Figure 7 shows the dependency of the efficiency  $\eta_h$  and the cavitation parameter  $\sigma_s$  on the net head  $H$ . The best efficiency point (BEP) is achieved for OP5. The efficiency drops significantly if the net head drops below 11 m. The value of the cavitation parameter  $\sigma_s$  is the lowest for OP3. With a decreasing net head, the  $\sigma_s$  value increases slightly. With increasing net head, the  $\sigma_s$  value increases significantly.

The precise CFD evaluation of the cavitation pa-

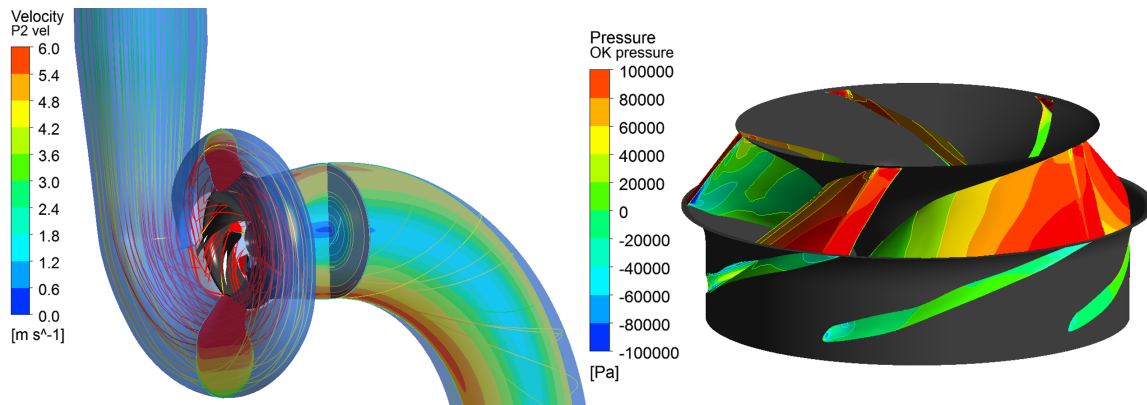


FIGURE 8. CFD results for the best efficiency point – the contour of absolute velocity (left) and pressure contours of the runner (right).

parameter  $\sigma_s$  is quite problematic. Our procedure is based on a static evaluation of the given pressures on the runner blades [17, 18]. This procedure proved successful in optimising Kaplan-type turbines [19]. We acknowledge that, in comparison to the efficiency evaluation, the evaluation of the cavitation parameter may exhibit a significant margin of error and requires further validation. Especially problematic for pressure behaviour and latter  $\sigma_s$  evaluation is the blade suction side area near the leading edges (Figure 8 – right). Left side of Figure 8 shows a longitudinal section with both absolute velocity and streamlines at the same time.

## 7. CONCLUSION

The study highlighted the potential of using an affordable scanning solution (Intel RealSense Lidar L515, Depth Camera D455 and Depth Camera D405) for a particular PAT unit. The 3D scanning, and especially the surface reconstruction, was the most time-consuming part of the process. There were many adjustments to the 3D scan and model settings for the final model to be as representative as possible. The CFD model could not be validated due to the impossibility of quality turbine performance measurement. All settings of the CFD model correspond to the best in-house validations, best practice recommendations, and findings from the scientific literature. For similar microturbines, we are used to an error of hydraulic efficiency in the CFD model of around 2–3% in BEP. Uncertainties are expected to be slightly higher due to the inaccuracies in scanning for this specific turbine. For future investigations, the most important is to prioritise high-quality measurements (if it is possible) to validate the CFD model adequately and to reduce uncertainty regarding outputs of the numerical model.

In the case of the demonstrated PAT turbine, a preliminary design has been proposed for a new runner and adjustments to the design of the turbine. The proposed design will serve as the basis for a multi-criteria CFD optimisation, focusing on optimising the turbine efficiency ( $\eta_h$ ) and the cavitation parameter

( $\sigma_s$ ). With the CFD shape optimisation, designing tailor-made turbines to achieve maximum energy production or the highest financial profit is possible.

## ACKNOWLEDGEMENTS

This research was funded by Student Grant Competition of CTU – SGS23/102/OHK1/2T/11 Reverse Engineering of Micro Hydro Turbines.

## REFERENCES

- [1] M. C. Morani, M. Simao, I. Gazur, et al. Pressure drop and energy recovery with a new centrifugal micro-turbine. *Energies* **15**(4):1528, 2022. <https://doi.org/10.3390/en15041528>
- [2] M. Binama, W.-T. Su, X.-B. Li, et al. Investigation on pump as turbine (PAT) technical aspects for micro hydropower schemes. *Renewable and Sustainable Energy Reviews* **79**:148–179, 2017. <https://doi.org/10.1016/j.rser.2017.04.071>
- [3] J. C. Alberizzi, M. Renzi, A. Nigro, M. Rossi. Study of a Pump-as-Turbine (PaT) speed control for a Water Distribution Network (WDN) in South-Tyrol subjected to high variable water flow rates. *Energy Procedia* **148**:226–233, 2018. <https://doi.org/10.1016/j.egypro.2018.08.072>
- [4] K. Çelebioğlu, A. Kaplan. Development and implementation of a methodology for reverse engineering design of Francis turbine runners. *Pamukkale University Journal of Engineering Sciences* **25**(4):430–439, 2019. <https://doi.org/10.5505/pajes.2018.43959>
- [5] J. Xu, L. Wang, S. N. Asomani, et al. Improvement of internal flow performance of a centrifugal pump-as-turbine (PAT) by impeller geometric optimization. *Mathematics* **8**(10):1714, 2020. <https://doi.org/10.3390/math8101714>
- [6] A. Breitbarth, C. Hake, G. Notni. Measurement accuracy and practical assessment of the lidar camera Intel RealSense L515. In *Optical Measurement Systems for Industrial Inspection XII*, vol. 11782, p. 1178213. SPIE, 2021. <https://doi.org/10.1117/12.2592570>
- [7] M. Servi, E. Mussi, A. Profili, et al. Metrological characterization and comparison of D415, D455, L515 realsense devices in the close range. *Sensors* **21**(22):7770, 2021. <https://doi.org/10.3390/s21227770>

- [8] M. Hrková, P. Koleda. Application of selected reverse engineering procedures based on specific requirements. *Multidisciplinary Aspects of Production Engineering* **4**(1):75–85, 2021. <https://doi.org/10.2478/mape-2021-0007>
- [9] F. D. Paola, T. Ingrassia, M. L. Brutto, A. Mancuso. A reverse engineering approach to measure the deformations of a sailing yacht. In *Advances on Mechanics, Design Engineering and Manufacturing*, pp. 555–563. Springer International Publishing, Cham, 2017. [https://doi.org/10.1007/978-3-319-45781-9\\_56](https://doi.org/10.1007/978-3-319-45781-9_56)
- [10] *IEC 62006:2010*. Geneva, edition 1.0 edn., 2010.
- [11] H. K. Versteeg, W. Malalasekera. *An introduction to computational fluid dynamics*. Pearson Prentice Hall, Harlow, 2nd edn., 2007.
- [12] I. B. Celik. Procedure for estimation and reporting of uncertainty due to discretization in CFD applications. *Journal of Fluids Engineering* **130**(7):4, 2008. <https://doi.org/10.1115/1.2960953>
- [13] P. J. Roache. Perspective. *Journal of Fluids Engineering* **116**(3):405–413, 1994. <https://doi.org/10.1115/1.2910291>
- [14] O. Petit, B. Mulu, H. Nilsson, M. Cervantes. Comparison of numerical and experimental results of the flow in the U9 Kaplan turbine model. *IOP Conference Series: Earth and Environmental Science* **12**:012024, 2010. <https://doi.org/10.1088/1755-1315/12/1/012024>
- [15] F. R. Menter. Two-equation eddy-viscosity turbulence models for engineering applications. *AIAA Journal* **32**(8):1598–1605, 1994. <https://doi.org/10.2514/3.12149>
- [16] P. E. Smirnov, F. R. Menter. Sensitization of the SST turbulence model to rotation and curvature by applying the spalart-shur correction term. *Volume 6: Turbomachinery, Parts A, B, and C* pp. 2305–2314, 2008. <https://doi.org/10.1115/GT2008-50480>
- [17] H. Benigni, H. Jaberg, J. Schiffer. Numerical simulation and optimisation of powerplant equipment with project realisation. In *Conference: Vienna HydroAt: Laxenburg/Wien*, p. 10. 2010.
- [18] A. Mundet, V. H. Hidalgo, X. Escaler. Numerical simulation of cavitation in a Francis runner under different operating conditions. In *International Symposium of Cavitation and Multiphase Flow. "The 3rd International Symposium of Cavitation and Multiphase Flow Shanghai, China, April 19th-22nd, 2019 ISCM2019: accepted abstracts, full papers"*, pp. 1–8. Shanghai University Press, Shanghai, 2019.
- [19] M. Kantor, M. Chalupa, J. Souček, et al. Application of genetic algorithm methods for water turbine blade shape optimization. *Manufacturing Technology* **20**(4):453–458, 2020. <https://doi.org/10.21062/mft.2020.072>